



Synthesis and Cr adsorption of a super-hydrophilic polydopamine-functionalized electrospun polyacrylonitrile

Xu Yang¹ · Yuhong Zhou¹ · Zhaojie Sun¹ · Chunhui Yang¹ · Dongyan Tang¹

Received: 10 May 2020 / Accepted: 21 August 2020 / Published online: 1 September 2020
© Springer Nature Switzerland AG 2020

Abstract

Electrospun fibers are advanced supporting layers in water purification. Coating the fibers with polydopamine should increase the hydrophilicity and removal efficiency. Here, we report a simple method to fabricate an adsorbent based on polydopamine and electrospun fibers. Polyacrylonitrile and dopamine coelectrospun micro-/nanofibers were selected as supporting layer, and then self-polymerization of polydopamine was used to functionalize the fibers. The polyacrylonitrile/polydopamine micro-/nanofibers were characterized by scanning electron microscopy (SEM), Fourier transform infrared (FTIR) and contact angle. Hexavalent chromium Cr(VI) was then used to investigate the adsorption by fabricated fibers. Results show that the fibers display a super-hydrophilicity and relative excellent adsorption capacity q_m of 61.65 mg g⁻¹ of Cr(VI). This finding is explained by the occurrence of amino and hydroxyl groups of polydopamine, and by the porous fibrous morphology of the electrospinning.

Keywords Electrospinning · Polydopamine coatings · Electrospun fibers · Adsorption · Cr(VI) removal

Introduction

The removal of contaminants and the fabrication of novel and valuable adsorbents are both of great significance to ensure the safety of drinking water (He et al. 2020). The strategy of membrane adsorption, with characteristics of relatively easy operation and higher separation efficiency, has attracted more attention in the field of water purification (Dharupaneedi et al. 2019; Chen et al. 2019). Thereinto, polymer-based adsorptive membranes, owing to high mechanical properties, good stability (especially the stability that within aqueous media) and excellent corrosion resistance, are more suitable for removing contaminants from aqueous media (Bao et al. 2019; Foster et al. 2020).

Electrospinning technique, a typical and efficient method for assembling nanofibrous polymer membranes, has been

used to fabricate novel and effective adsorbents. The widely used polymers included polyacrylonitrile, poly(vinylidene fluoride) and polyurethane (Mohamed et al. 2019; Liao et al. 2018; Mishra et al. 2019), and fabricated membranes would usually exhibit porous structures with adjustable porosity and other peculiar characters, such as higher water stability, good chemical durability and mechanical properties (Suja et al. 2017; Ge et al. 2018). Hence, the electrospun polymer fibers could be potentially used as the supporting layer to further prepare composite membranes with high-performance and satisfactory water flux. In addition, hydrophobic polymer membranes suffered easily fouled feature by bacteria or protein, resulting in an obvious reduction in the adsorption and filtration efficiency (Zhai et al. 2020). Through blending or modifying with hydrophilic agents, the hydrophilicity of the polymer membranes could be improved available (Huang et al. 2018; Chauque et al. 2016).

Besides the selection of suitable polymer and the designing of peculiar morphology, introducing effective adsorptive sites into this system might be available to improve its adsorptive abilities (Zhao et al. 2017; Zeytuncu et al. 2018). As a potential and green route to modify and functionalize the surface of material, self-polymerization of bio-inspired dopamine to form polydopamine coatings would couple with the surface of such interactions

Electronic supplementary material The online version of this article (<https://doi.org/10.1007/s10311-020-01086-7>) contains supplementary material, which is available to authorized users.

✉ Dongyan Tang
dytang@hit.edu.cn

¹ School of Chemistry and Chemical Engineering, Harbin Institute of Technology, Harbin 150001, China

as covalent bond and show relative stronger adhesion and better stability (Zhang et al. 2020a, b; Dreyer et al. 2013). Moreover, polydopamine-functionalized surfaces with several advantages of lower cost, nontoxic and adaptable in chemical environment, have been widely studied as water purification membranes and enzymatic carrier, and showed great potential in the fields of tissue engineering, gene delivery, batteries, sensor, catalysts, and so on (Ahmad, et al. 2020; Zhang, et al. 2020a, b). Particularly, due to the existence of plentiful amine groups, polydopamine coatings could further improve the adsorption performance, hydrophilicity and the water flux of polymeric membrane during the usage in water treatment.

In this work, the electrospun polyacrylonitrile/dopamine micro-/nanofibers were fabricated as support membrane, and then green and nontoxic polydopamine coating was introduced onto the surface of fibers to improve the hydrophilicity and the adsorption performance. Combining electrospinning technique and self-polymerization method, the composite fibrous membranes of polyacrylonitrile/polydopamine were facily prepared by two steps. The micromorphology, structures, hydrophilicity and hexavalent chromium (Cr(VI)) adsorption abilities and adsorption mechanics of polyacrylonitrile/polydopamine were all investigated in detail.

Experimental section

Materials and preparation of micro-/nanofibers

The details of the used chemicals are described in the Supporting Information, and the chemicals were used directly without recrystallization. Typically, 0.14 g of dopamine and 0.28 g of polyacrylonitrile were dissolved in 1.72 g of *N,N*-dimethylformamide to form a homogeneous spinning solution. Then, the spinning solution was loaded into a 2.5-mL syringe (with a 0.84-mm-diameter nozzle), and the electrospinning process was carried out at a feeding rate of 0.1 mL h⁻¹, a collecting distance of 15 cm and a voltage of 19 kV at room temperature.

Subsequently, the as-prepared polyacrylonitrile/dopamine micro-/nanofibers were immersed into 100 mL of dopamine HCl (2 g L⁻¹) at a pH value of 8.5. Then, for different periods of time (0–30 h), the fibers were taken out, washed and dried at 80 °C overnight. The sample was denoted as polyacrylonitrile/polydopamine-*x* (PAN/PDA-*x*), where *x* referred to the polymerization time (h) of polydopamine. Characterization, instruments and the detailed preparation procedures of pure polyacrylonitrile and polydopamine-coated polyacrylonitrile micro-/nanofibers are described in Supporting Information.

Cr(VI) removal experiments and adsorption detections

Polyacrylonitrile/polydopamine micro-/nanofibers (20 mg) were immersed into a solution of Cr(VI) (20 mL) for different period of times, and the concentration of Cr(VI) was determined with 1,5-diphenyl carbazide and spectrophotometric method, which was measured by a an ultraviolet–visible spectrometer (760 CRT, INEAA, China) at 540 nm. Then, the adsorption capacity was calculated by Equations S1 and S2.

Results and discussion

Morphology, structures and hydrophilic of polyacrylonitrile/polydopamine micro-/nanofibers

Comparison with pure polyacrylonitrile micro-/nanofibers (Fig. 1a) and polydopamine-coated polyacrylonitrile micro-/nanofibers exhibited a thin covered layer onto the surface of the fibers, and the porous structures were blocked partially with the disappearance of the fibrous morphology to some extent (Fig. 1b) (Ma et al. 2018). In order to avoid such phenomenon, to guarantee the uniform distribution of polydopamine across the single fiber and to maintain the fibrous morphology, mostly, polyacrylonitrile/polydopamine fibers were fabricated by combining the coelectrospinning of polyacrylonitrile/dopamine and the self-polymerization of dopamine (Fig. 1c).

Different from the relatively smooth surface of polyacrylonitrile/dopamine (Figure S1), the morphology of polyacrylonitrile/polydopamine showed a relatively coarse surface with observable particles (as shown in Fig. 2a–h). Furthermore, upon prolonging the self-polymerization times of polydopamine, more and obvious particles could be formed with stacked or agglomerated states on the surface of fibers, and it could cause the increased roughness of the fibers. Therefore, polyacrylonitrile/polydopamine micro-/nanofibers exhibited obvious porous and fibrous states with the uniform distribution of polydopamine coatings on the surfaces. Moreover, as shown in Fig. 2i, after coating by polydopamine, the color of the membranes changed gradually (from the original white to gray, and to dark black after 5-h treatment). The obvious changes in colors might be resulted from the self-polymerization of polydopamine (Son et al. 2013), which indicated the successful and rapid fabrication of novel fibers based on polyacrylonitrile and polydopamine by simple synthesized approaches.

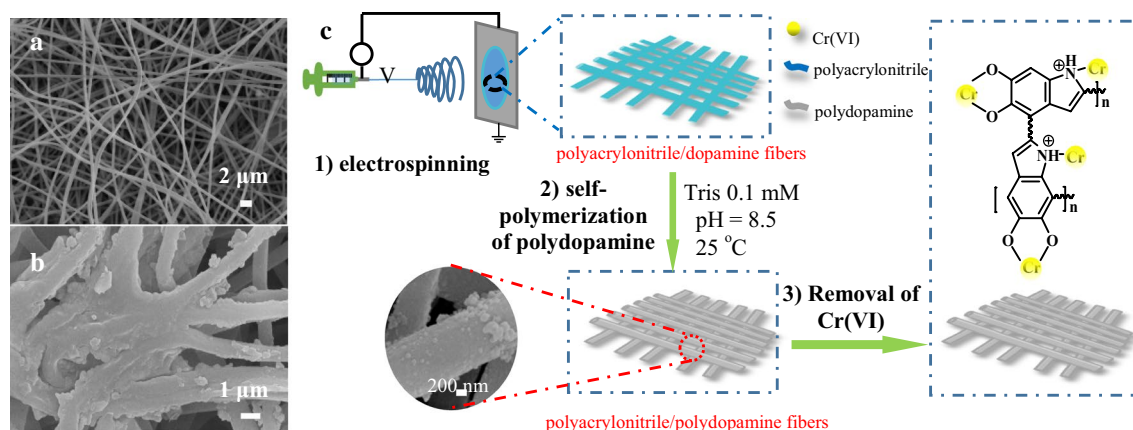


Fig. 1 Scanning electron microscopy (SEM) images of **a** polyacrylonitrile and **b** polydopamine-coated polyacrylonitrile; **c** preparation procedures of polyacrylonitrile/dopamine by electrospinning (1); the

further polyacrylonitrile/polydopamine by self-polymerization of dopamine (2); and the removal of Cr(VI) (3)

Fourier transform infrared (FTIR) spectra of a series of polyacrylonitrile/polydopamine are represented in Fig. 2j. The broad peak at around 3313 cm^{-1} was ascribed to the stretching vibration of $-\text{OH}$, while peaks at 2240 , 1600 and 1246 cm^{-1} were assigned to the stretching vibration of $-\text{CN}$ within polyacrylonitrile, $\text{C}-\text{O}$ and aromatic benzene ring within polydopamine, respectively (Wu et al. 2017). Moreover, increasing the self-polymerization times, the relative intensities of peaks at 3313 and 1600 cm^{-1} increased and the contents of polydopamine within polyacrylonitrile/polydopamine increased gradually, confirming the self-polymerization of polydopamine on the surface of the fibers (Ma et al. 2017).

Here, the contact angle of ultra-water on the fibers was detected and used to evaluate the hydrophilicity of the fibers (as shown in Fig. 2k). The contact angle of polyacrylonitrile was 106° with stable values, indicating the hydrophobicity of polyacrylonitrile micro-/nanofibers. Whereas, the contact angle of polyacrylonitrile/dopamine decreased gradually from 28° to 0° , indicating the hydrophilicity. Moreover, super-hydrophilicity polyacrylonitrile/polydopamine could be wetted by ultra-water within the contact time of one second (the contact angle was 0°). That meant, owing to the existence of large amount of hydrophilic groups (amino and hydroxyl) within polydopamine structures, the self-polymerization of polydopamine on the surface of the fibers could increase the surface charge density, and further increase the hydrophilicity (Koopal 2012). In addition, by the increase in hydrophilicity, the water fluxes of polyacrylonitrile/polydopamine could be increased after the modification of polydopamine (as shown in Figure S2), which was attributed to the improvement in the permeability of micro-/nanofibers by the hydrophilic polydopamine (Zhan et al. 2018).

The removal capacity and the adsorption isotherms

In this work, Cr(VI) was selected as the target adsorbate to detect the adsorption performance of the fabricated fibers. The equilibrium adsorption capacity (q_e) of polyacrylonitrile was 9.47 mg g^{-1} (as shown in Figure S3). After the modification of polydopamine, polyacrylonitrile/polydopamine exhibited remarkably increased adsorption capacity toward Cr(VI) (Fig. 3a). Increasing the self-polymerization times, the values of q_e increased obviously with the maximum values for that polyacrylonitrile/polydopamine-20 up to 49.01 mg g^{-1} . Hence, the dramatically improved adsorption performance by the coating of polydopamine due to the provided active sites by polydopamine. Moreover, as shown in Figure S4, the value of q_e of 35.25 mg g^{-1} for polydopamine-coated polyacrylonitrile was less than that of polyacrylonitrile/polydopamine, indicating that the blocking of the porous structures would reduce the efficiency of active sites and the water flux, thus further decreasing the adsorption performance of the membranes. Therefore, combining the effects of the fibrous morphology and the introduction of active sites by polydopamine, the efficient adsorption of polyacrylonitrile/polydopamine micro-/nanofibers could be achieved effectively.

Then, the adsorption isotherms were simulated by Langmuir and Freundlich models (Equations S3 and S4). As shown in Fig. 3b and c, comparing the values of R^2 (the correlation coefficients), the adsorption data of Cr(VI) obeyed the Langmuir model. It could be deduced that the active sites were widely distributed on the surface of polyacrylonitrile/polydopamine micro-/nanofibers, and the adsorption process was mainly controlled by the monolayer adsorption. Besides, calculated by the Langmuir model, the maximum adsorption capacity (q_m) of polyacrylonitrile/polydopamine was about

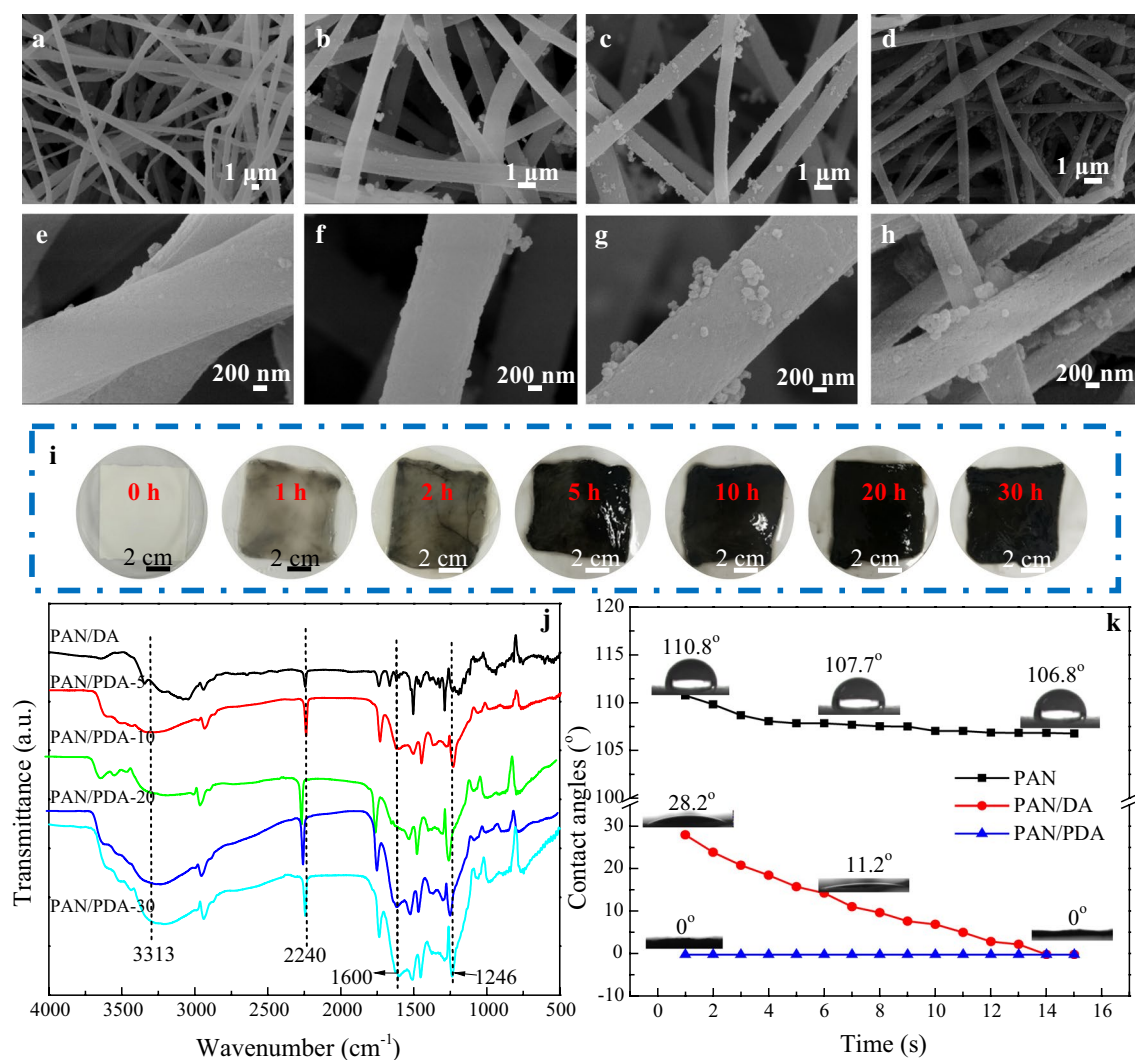


Fig. 2 Scanning electron microscopy (SEM) morphological images of fibers, which are taken at relatively low (a–d) and high magnifications (e–h); a and e polyacrylonitrile/polydopamine-5; b and f polyacrylonitrile/polydopamine-10; c and g polyacrylonitrile/polydopamine-20; d and h polyacrylonitrile/polydopamine-30; i the digital photographs of polyacrylonitrile/polydopamine with different

self-polymerization times; j FTIR spectra of polyacrylonitrile/dopamine and polyacrylonitrile/polydopamine; and k the comparison of the contact angle of ultra-pure water on the surfaces of the different micro-/nanofibers with the increasing times; the abbreviations in figures are explained as follows: PAN/PDA polyacrylonitrile/polydopamine, PAN/DA polyacrylonitrile/dopamine, PAN polyacrylonitrile

61.65 mg g⁻¹ and that was comparable or superior to some reported adsorbents (as shown in Table 1).

Furtherly, to investigate the applicable stability of the fabricated fibrous membranes within aqueous media, and to confirm the distribution of the active sites onto the fibers, polyacrylonitrile/polydopamine-20 was selected to have the SEM observations, and the related elemental mapping scanning images after being adsorbed for 8 h are shown in Fig. 3g–i. The unobvious changing of the morphology indicated the good water stability of polyacrylonitrile/polydopamine micro-/nanofibers. Furthermore, the elemental mapping images showed the homogeneous distribution of the elements (Cr and C), demonstrating the self-polymerization

of polydopamine underwent uniformly on the surface of the fibers, and thus, the following adsorption of Cr(VI) could be guaranteed evenly on the surface of the fibrous membrane.

Adsorption thermodynamics and adsorption kinetics

For polyacrylonitrile/polydopamine-20, the adsorption of Cr(VI) was conducted under different temperatures, and the results are shown in Figure S5. The adsorption capacity increased gradually with the increasing temperatures. Then, the thermodynamic parameters of standard Gibbs free energy change (ΔG°), enthalpy change (ΔH°) and entropy

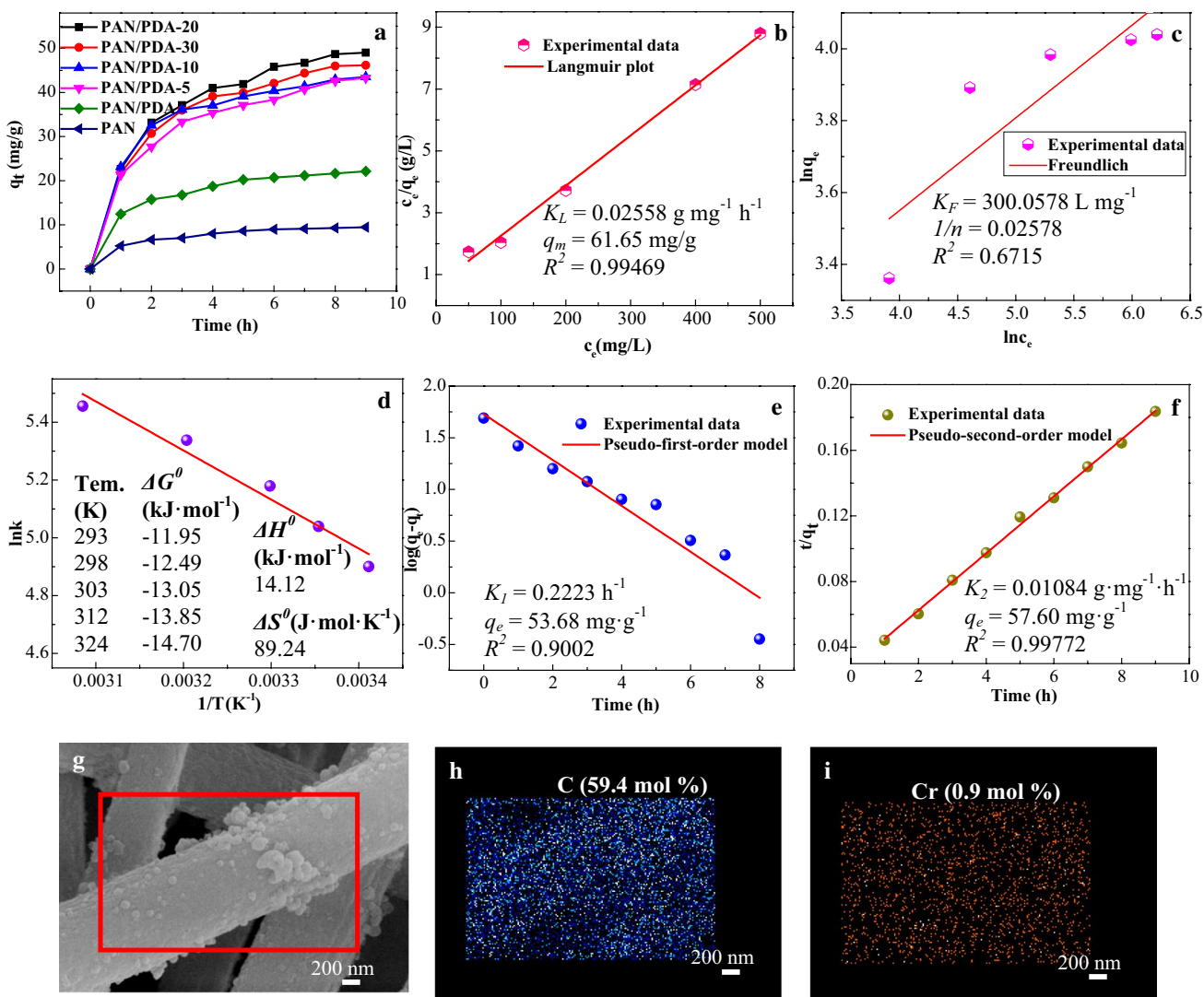


Fig. 3 **a** Comparison of Cr(VI) adsorption amounts for different polyacrylonitrile/polydopamine as indicated with the increasing adsorption times; **b** the Langmuir isothermal model and **c** the Freundlich isothermal model for the adsorption of Cr(VI); **d** the plot of $\ln K$ versus $1/T$ to determine the thermodynamic parameters; **e** the pseudo-

first-order kinetic model and **(f)** the pseudo-second-order kinetic model for the adsorption of Cr(VI); **g** SEM images of the adsorption of Cr(VI) on the sample of polyacrylonitrile/polydopamine-20; **h** and **i** the elemental mapping images for elements of C and Cr, respectively

Table 1 The comparison of the adsorption capacity of Cr(VI) by different adsorbents

Adsorbent	q_m (mg g ⁻¹)	References
Modified peach stone	24.68	Lan et al. (2019)
Chitosan-combined magnetic biochars	30.14	Xiao et al. (2019)
Nano UiO-66-NH ₂ Metal-organic frameworks	32.36	Wu et al. (2018)
Polystyrene/thermoplastic polyurethane@SiO ₂ microfiber membrane	57.73	Wang et al. (2019)
Morphology-controlled synthesis of boehmite	64.70	Li et al. (2019)
Polyacrylonitrile/polydopamine micro-/nanofibers	61.65	This work

change (ΔS°) were all calculated by Equations S5 and S6 and given in Fig. 3d. The negative values of ΔG° decreased with the increasing temperatures, indicating the spontaneous

process of the adsorption, and thus, increasing the temperatures would be a beneficial way to adsorption. In addition, the positive values of ΔS° (89.24 J mol⁻¹ K⁻¹) and ΔH°

(14.12 kJ mol⁻¹) further confirmed the endothermic process for the adsorption, and the process would be promoted by the heating treatment.

Moreover, by the well-known pseudo-first-order adsorption model and pseudo-second-order adsorption model (Equations S7 and S8), the adsorption kinetics were investigated and the results are shown in Fig. 3e, f. Thereinto, the value of R^2 of the pseudo-second-order model (0.9977) was higher than that of the pseudo-first-order model (0.9002), the calculated value of q_e by the pseudo-second-order model was more fitting to the experimental data, and the value of K_2 was larger than that of K_1 . These results indicated that the adsorption process toward Cr(VI) was matched better with the pseudo-second-order model. Therefore, a chemical process was the leading role during the adsorption process, which was related to the electrons sharing or transferring between the adsorbent and the adsorbate.

Changing the pH values of the adsorbent solution would influence the adsorption process through governing the protonation of adsorbents and simultaneously adjusting the capacities of different Cr(VI) species (as shown in Table S1). Thus, the effect of pH values on the adsorption capacity was further investigated under the pH ranges of 3.0–11.0 (as shown in Figure S6). The values of q_e increased steadily with the decrease in pH values, owing to the full protonated forms of the amino and hydroxyl groups, and to the promoting of the attraction to negative Cr(VI) species. While at a lower pH value of 3.0, the adsorption capacity reduced due to the disappearance of protonation and the formation of neutral Cr(VI) species. On the base of the previous references and the above results (Zhang et al. 2018), the adsorption mechanism of Cr(VI) onto polyacrylonitrile/polydopamine might be driven by electrostatic interaction and complexation (as shown in Fig. 1c). In conclusion, combining the advantages of electrospun polyacrylonitrile fibers and self-polymerization of polydopamine, polyacrylonitrile/polydopamine micro-/nanofibers exhibited porous and fibrous morphology with large amounts of the attached functional groups (including amino and hydroxyl from polydopamine coatings); thus, it would be potentially applied in heavy metal ions adsorption.

Conclusion

A new adsorbent based on hydrophobic polyacrylonitrile and hydrophilic polydopamine has been successfully fabricated, via coelectrospinning of polyacrylonitrile and dopamine, following by self-polymerization of polydopamine onto the fibrous surface. The obtained polyacrylonitrile/polydopamine micro-/nanofibers displayed a porous and fibrous morphology with homogeneous polydopamine coatings. Besides, polyacrylonitrile/polydopamine exhibited fibers'

well water stability and surfaces' super-hydrophilicity simultaneously. Then, the fibers were applied to removal of Cr(VI) experiments and shown good adsorption capacity (q_m of 61.65 mg g⁻¹), which was comparable or superior to some reported adsorbents. Thus, polyacrylonitrile/polydopamine micro-/nanofibers with higher flexibility, water stability and excellent adsorption performance could be facilely synthesized and potentially applied in wastewater treatment.

Acknowledgments The authors are grateful to the Excellent Academic Leaders Foundation of Harbin, China (No. 2014RFXXJ017).

References

- Ahmad T, Byun H, Lee J, Perikamana SKM, Shin YM, Kim EM, Shin H (2020) Stem cell spheroids incorporating fibers coated with adenosine and polydopamine as a modular building blocks for bone tissue engineering. *Biomaterials* 230:54
- Bao X, Wu Q, Shi W, Wang W, Yu H, Zhu Z, Zhang X, Zhang Z, Zhang R, Cui F (2019) Polyamidoamine dendrimer grafted forward osmosis membrane with superior ammonia selectivity and robust antifouling capacity for domestic wastewater concentration. *Water Res* 153:1–10
- Chauque EFC, Dlamini LN, Adelodun AA, Greyling CJ, Ngila JC (2016) Modification of electrospun polyacrylonitrile nanofibers with EDTA for the removal of Cd and Cr ions from water effluents. *Appl Surf Sci* 369:19–28
- Chen W, Mo J, Du X, Zhang Z, Zhang W (2019) Biomimetic dynamic membrane for aquatic dye removal. *Water Res* 151:243–251
- Dharupaneedi SP, Nataraj SK, Nadagouda M, Reddy KR, Shukla SS, Aminabhavi TM (2019) Membrane-based separation of potential emerging pollutants. *Sep Purif Technol* 210:850–866
- Dreyer DR, Miller DJ, Freeman BD, Paul DR, Bielawski CW (2013) Perspectives on poly(dopamine). *Chem Sci* 4:3796–3802
- Foster JC, Starstrom SA, DeVol TA, Powell BA, Husson SM (2020) Functionalized polymer thin films for plutonium capture and isotopic screening from aqueous sources. *Anal Chem*
- Ge J, Zong D, Jin Q, Yu J, Ding B (2018) Biomimetic and superwetable nanofibrous skins for highly efficient separation of oil-in-water emulsions. *Adv Funct Mater* 28:10
- He C, Gu L, Xu Z, He H, Fu G, Han F, Huang B, Pan X (2020) Cleaning chromium pollution in aquatic environments by bioremediation, photocatalytic remediation, electrochemical remediation and coupled remediation systems. *Environ Chem Lett* 18:561–576
- Huang M, Tu H, Chen J, Liu R, Liang Z, Jiang L, Shi X, Du Y, Deng H (2018) Chitosan-rectorite nanospheres embedded aminated polyacrylonitrile nanofibers via shoulder-to-shoulder electrospinning and electrospinning for enhanced heavy metal removal. *Appl Surf Sci* 437:294–303
- Koopal LK (2012) Wetting of solid surfaces: fundamentals and charge effects. *Adv Colloid Interface* 179:29–42
- Lan G, Zhang Y, Liu Y, Qiu H, Liu P, Yan J, Zhang T (2019) Modified peach stones by ethylenediamine as a new adsorbent for removal of Cr(VI) from wastewater. *Sep Sci and Technol* 54:2126–2137
- Li J, Li M, Yang X, Zhang Y, Liu X, Liu F, Meng F (2019) Morphology-controlled synthesis of boehmite with enhanced efficiency for the removal of aqueous Cr(VI) and nitrates. *Nanotechnology* 30:12
- Liao Y, Loh CH, Tian M, Wang R, Fane AG (2018) Progress in electrospun polymeric nanofibrous membranes for water treatment: fabrication, modification and applications. *Prog Polym Sci* 77:69–94

- Ma FF, Zhang N, Wei X, Yang JH, Wang Y, Zhou ZW (2017) Blend-electrospun poly(vinylidene fluoride)/polydopamine membranes: self-polymerization of dopamine and the excellent adsorption/separation abilities. *J Mater Chem A* 5:14430–14443
- Ma FF, Zhang D, Zhang N, Huang T, Wang Y (2018) Polydopamine-assisted deposition of polypyrrole on electrospun poly(vinylidene fluoride) nanofibers for bidirectional removal of cation and anion dyes. *Chem Eng J* 354:432–444
- Mishra RK, Mishra P, Verma K, Mondal A, Chaudhary RG, Abolhasani MM, Loganathan S (2019) Electrospinning production of nanofibrous membranes. *Environ Chem Lett* 17:767–800
- Mohamed A, Ghobara MM, Abdelmaksoud MK, Mohamed GG (2019) A novel and highly efficient photocatalytic degradation of malachite green dye via surface modified polyacrylonitrile nanofibers/biogenic silica composite nanofibers. *Sep Purif Technol* 210:935–942
- Son HY, Ryu JG, Lee H, Nam YS (2013) Silver-polydopamine hybrid coatings of electrospun poly(vinyl alcohol) nanofibers. *Macromol Mater Eng* 298:547–554
- Suja PS, Reshmi CR, Sagitha P, Sujith A (2017) electrospun nanofibrous membranes for water purification. *Polym Rev* 57:467–504
- Wang B, Sun Z, Liu T, Wang Q, Li C, Li X (2019) NH₂-grafting on micro/nano architecture designed PS/TPU@SiO₂ electrospun microfiber membrane for adsorption of Cr(VI). *Desalin Water Treat* 154:82–91
- Wu F, Pu N, Ye G, Sun T, Wang Z, Song Y, Wang W, Huo X, Lu Y, Chen J (2017) Performance and Mechanism of Uranium Adsorption from Seawater to Poly(dopamine)-Inspired Sorbents. *Environ Sci Technol* 51:4606–4614
- Wu S, Ge Y, Wang Y, Chen X, Li F, Xuan H, Li X (2018) Adsorption of Cr(VI) on nano UiO-66-NH₂ MOFs in water. *Environ Technol* 39:1937–1948
- Xiao F, Cheng J, Cao W, Yang C, Chen J, Luo Z (2019) Removal of heavy metals from aqueous solution using chitosan-combined magnetic biochars. *J Colloid Interf Sci* 540:579–584
- Zeytuncu B, Urper M, Koyuncu I, Tarabara VV (2018) Photocrosslinked PVA/PEI electrospun nanofiber membranes: preparation and preliminary evaluation in virus clearance tests. *Sep Purif Technol* 197:432–438
- Zhai WT, Wang ML, Song JF, Zhang L, Li XM, He T (2020) Fouling resistance of 3-3-(trimethoxysilane)-propyl amino propane-1-sulfonic acid zwitterion modified poly(vinylidene fluoride) membranes. *Sep Purif Technol* 239:489
- Zhan Y, Wan X, He S, Yang Q, He Y (2018) Design of durable and efficient poly(arylene ether nitrile)/bioinspired polydopamine coated graphene oxide nanofibrous composite membrane for anionic dyes separation. *Chem Eng J* 333:132–145
- Zhang Q, Li Y, Yang Q, Chen H, Chen X, Jiao T, Peng Q (2018) Distinguished Cr(VI) capture with rapid and superior capability using polydopamine microsphere: behavior and mechanism. *J Hazard Mater* 342:732–740
- Zhang GQ, Zheng GL, Ren TH, Zeng XQ, Heide E (2020a) Dopamine hydrochloride and carboxymethyl chitosan coatings for multifilament surgical suture and their influence on friction during sliding contact with skin substitute. *Friction* 8:58–69
- Zhang P, Xu QN, Li XF, Wang YX (2020b) pH-responsive polydopamine nanoparticles for photothermally promoted gene delivery. *Mat Sci Eng C Mater* 108:32
- Zhao R, Li X, Sun B, Ji H, Wang C (2017) Diethylenetriamine-assisted synthesis of amino-rich hydrothermal carbon-coated electrospun polyacrylonitrile fiber adsorbents for the removal of Cr(VI) and 2,4-dichlorophenoxyacetic acid. *J Colloid Interf Sci* 487:297–309

Publisher's Note Springer Nature remains neutral with regard to jurisdictional claims in published maps and institutional affiliations.